

许慧君先生论文集

(第三册)

中国科学院感光化学研究所

2000 年 7 月

许慧君先生论文集

(第三册)

KG16/04
(KG16/37)

中国科学院感光化学研究所

2000 年 7 月

江苏工业学院图书馆
藏书章

Charge-separated-state enhancement of the third-order optical nonlinearity of a photosensitizer-electron acceptor triad assembly

Jinhai Si¹, Yougui Wang¹, Qiguang Yang¹, Peixian Ye¹, Hongjian Tian², Qingfu Zhou², Huijun Xu²

¹ Institute of Physics, Chinese Academy of Sciences, P.O. Box 603, Beijing 100080, P.R. China

² Institute of Photographic Chemistry, Chinese Academy of Sciences, Beijing, P.R. China

Received: 2 July 1996

Abstract. The molecular hyperpolarizability $\gamma(-\omega;\omega,\omega,-\omega)$ of a supramolecule, zinc 4,4',4'',4'''-tetrasulfonato-phthalocyanine/N-butyl-N'-methylantraquinone-4,4'-bipyridinium dibromide assembly (ZnTsPc-V-AQ), was observed to be enhanced by ten times when the sample was optically pumped by a 355 nm pump beam. The enhancement of the nonlinearity was found to be due predominantly to the charge transfer between the two monomers of the supramolecule after optical excitation.

PACS: 42.65.-k, 42.70.-h

Nonlinear optics is expected to play a major role in the technology of photonics. Recent progress in the field of high-speed optoelectronics and information technology has encouraged the search for materials with a large, fast nonlinear optical (NLO) response and for new ways to enhance this response [1]. A.F. Garito and colleagues have found a new way to achieve large $\chi^{(3)}$ through excited-state population [2], and the enhanced NLO process related to electronic excited states has been observed in some conjugated organic materials [3,4]. Then, the subject is turned to find those kinds of excited states which can effectively and intensively enhance the nonlinearities of the materials. It is well known that some compounds with an intramolecular charge transfer have large optical nonlinearities. For example, the metal–ligand bonding in organometallics gives rise to large molecular hyperpolarizabilities due to the transfer of electron density between the metal atom and conjugated ligand systems [5,6]. Therefore, if an excited state with an intramolecular charge transfer can be formed by optical excitation, we believe that when this excited state is populated, nonlinearities of the material will probably be enhanced.

It has been shown that the stacked and bridged porphyrin [7] or phthalocyanine [8] assemblies can exhibit unusual charge-transfer properties after optical excitation owing to the strong π – π interactions between the two macrocycles and the formation of exciton coupling in the sandwich complexes. An example that includes

a supramolecular configuration of a linked photosensitizer-electron acceptor(1)-electron acceptor(2), $S-A_1-A_2$, has been reported recently [9]. In this system an effective charge separation of the photoproducts ($S^+-A_1-A_2^-$) was obtained through photoexcitation of the sensitizer component (Fig. 1). Thus, this kind of supramolecular system can be used to investigate the influence of charge transfer caused by laser excitation on molecular hyperpolarizabilities.

In this paper, we report our studies on the nonlinearity of the light-induced charge separated (CS) state of the supramolecule, zinc 4,4',4'',4'''-tetrasulfonato-phthalocyanine/N-butyl-N'-methylantraquinone-4,4'-bipyridinium dibromide assembly (ZnTsPc-V-AQ). An increase in the degenerate-four-wave-mixing (DFWM) signal as large as two orders of magnitude was observed when the population of the CS state was saturated by a 355 nm pump beam. Our experiments indicate also that the nonlinearity of the CS state is predominantly electronic in origin.

1 Experimental

The supramolecular assembly consisting of electrostatically paired ZnTsPc-V-AQ is formed in the liquid phase by pairing one ZnTsPc⁴⁻ with two V²⁺-AQ. It is prepared by mixing ZnTsPc with V-AQ in a molar ratio of 1 : 2 in dimethylformamide (DMF), in which all of the ZnTsPc molecules can be almost assembled. ZnTsPc-V-AQ has two absorption bands that are similar to the absorption bands of ZnTsPc: the Q band ($\lambda_{\max} = 680$ nm) and the B band ($\lambda_{\max} = 340$ nm). ZnTsPc monomer fluoresces strongly; with the presence of the linked electron acceptors V-AQ, the fluorescence is quenched, indicating the existence of a very efficient electron transfer from

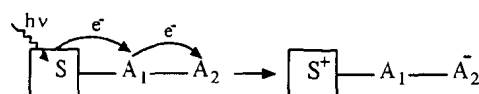


Fig. 1. Schematic vectorial electron transfer process in a linked photosensitizer-electron acceptor(1)-electron acceptor(2) molecular assembly

the ZnTsPc to the V-AQ. On the action of 355 nm pump beam, the sensitizer ZnTsPc in the ZnTsPc-V-AQ assembly is excited optically from the ground state to the second excited singlet state. It then relaxes very rapidly (0.1–10 ps) [7] to the CS state either directly or through the first excited singlet state. This charge-separation process is achieved by an electron transfer from the sensitizer ZnTsPc to the acceptor(2) Q through the acceptor(1) V. Molecules in the CS state with a short lifetime (0.1–1 ns) [7] will come back to the ground state by charge recombination.

In our experimental studies, a forward DFWM geometry with an additional pump beam was used [4]. The 8 ns, 1064 nm pulses from a Q-switch Nd:YAG laser were first doubled and then mixed in KD*P crystals to produce the third-harmonic pulses at 355 nm, which served as the pump beam to excite the system to the CS state. The remaining 1064 nm beam was split into two beams, which served as the probe beams to perform the DFWM experiment at the CS state. Two probe beams with wave-vectors k_1 and k_2 were focused in coincidence on the sample at a small angle of 1.5° . The pump beam was passed through an attenuator to allow adjustment of the beam intensity and was then also focused onto the interaction region in the sample cell, whose thickness was 2 mm. The diameter of the pump beam was ~ 0.6 mm; the probe beams had diameters of ~ 0.4 mm to ensure their overlap. The pump pulse and the two probe pulses also had temporal overlap. The diffracted signal in the $2k_2 - k_1$ direction was detected by a photomultiplier tube. No evident absorption in ZnTsPc-V-AQ at 1064 nm with or without the pump beam was observed.

2 Results and discussion

When ZnTsPc-V-AQ solution with a concentration of 3×10^{-3} M was pumped by the pump beam, enhancement of the DFWM signal was observed. At a saturation pump intensity, the signal was enhanced by two orders of magnitude. We also observed that the signals, both with and without the pump beam, had a expected cubic dependence on the probe intensities, which confirms that the signals arise from the third-order nonlinearity of the sample.

In general, third-order nonlinearities of the sample may be due to both electronic and nuclear orientation factors. When the polarization of the probe k_2 is changed from a parallel to a perpendicular orientation with respect to the polarization of the probe k_1 , the DFWM signal should drop by a factor of $(\chi_{xxx}^{(3)}/\chi_{xyx}^{(3)})^2 = 1/9$ for purely electronic hyperpolarizability and $9/16$ for purely orientation nonlinearity [10]. By measuring the ratio of the signals for the parallel and perpendicular probe polarizations, one can estimate the ratio of the orientation and electronic contributions. Our measurements show that for both cases of pump on and pump off, the signals for perpendicular probe polarizations were about $1/9$ of the signals for parallel probe polarizations, indicating that the DFWM signals originate entirely from the electronic, not the orientation and thermal, effects.

The DFWM signal with the pump on was measured as a function of the pump intensity for a ZnTsPc-V-AQ solution with a concentration of 1.23×10^{-3} M, as shown in Fig. 2. The signal shows a square pump-intensity dependence as expected, and shows evidence of saturation at high pump intensities. Hence it is verified that the enhanced signal is related to the

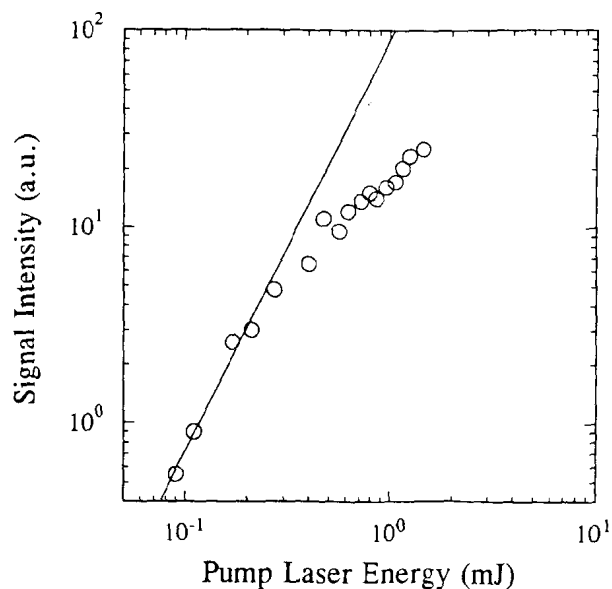


Fig. 2. Measured DFWM signal versus pump laser energy for ZnTsPc-V-AQ solution with a concentration of 1.23×10^{-3} M. The solid line is a square fit to the signal

population of an electronic excited state because the population has a linear dependence on the pump intensity. However, we cannot yet know whether the enhancement is due to population of the CS state or that of the second excited singlet state.

In order to verify that the enhancement of the nonlinearity arises from the CS state of ZnTsPc-V-AQ, DFWM signals of the samples with different molar ratios of V-AQ to ZnTsPc were measured at a fixed ZnTsPc concentration of 3.22×10^{-4} M and a pump intensity of 4.5×10^6 W/cm²; the results are shown in Fig. 3. With an increase in the molar ratio C_{V-AQ}/C_{ZnTsPc} , the signal decreases at first and then increases.

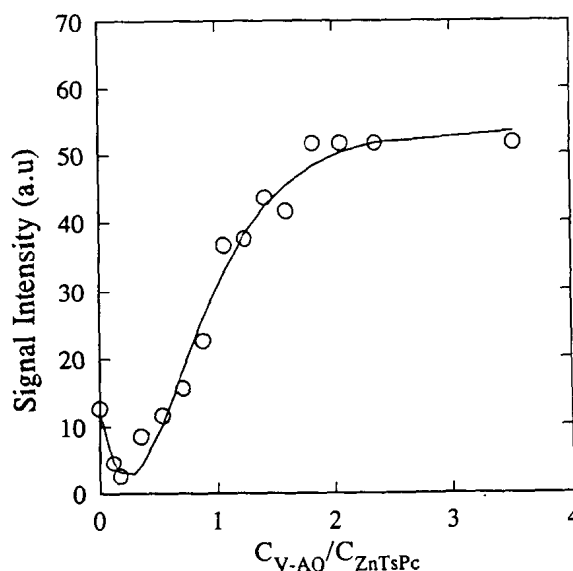


Fig. 3. DFWM signal versus the molar ratio of V-AQ to ZnTsPc measured at a fixed ZnTsPc concentration of 3.22×10^{-4} M and a pump intensity of 4.5×10^6 W/cm²

es. It also shows evidence of saturation for ratios larger than 2, indicating that the ZnTsPc molecules are almost all assembled at this ratio. In the absence of V-AQ or ZnTsPc, no obvious enhancement of the signals from both samples was observed. When the pump beam was turned off, the signal remained almost constant for different ratios. These results imply that the enhancement of the DFWM signal from ZnTsPc-V-AQ is due predominately to population of the CS state produced by the pump beam, not population of the second excited singlet state of ZnTsPc. In addition, the data in Fig. 3 show that the CS-state susceptibility $\chi_{CS}^{(3)}$ of ZnTsPc-V-AQ has an opposite sign to that of the sum of the susceptibilities of the solvent and the ground state of ZnTsPc, because a dip appears on the curve at the beginning. The third-order NLO susceptibility $\chi^{(3)}$ of ZnTsPc-V-AQ was determined in comparison with the measurements on a reference sample of CS₂ [11]. According to the above analysis, the electron-transfer process induced by the pump beam can be approximately treated as a two-level system, and the third-order NLO susceptibility with a pump beam can be written as

$$\chi^{(3)} = \chi_{\text{solvent}}^{(3)} + F(N_g \gamma^g + N_{CS} \gamma^{CS}), \quad (1)$$

where $\chi_{\text{solvent}}^{(3)}$ is the third-order NLO susceptibility of the solvent, F is the local field factor, γ^g and γ^{CS} are the molecular hyperpolarizabilities of the ground state and the CS state, respectively, and N_g and N_{CS} are the number densities of the ground state and the CS state, respectively. The γ^g for ZnTsPc-V-AQ was obtained from the measured values of $\chi_g^{(3)}$ for several different concentration samples.

In order to determine γ^{CS} the macroscopic $\chi^{(3)}$ as a function of concentration was measured. As an example, the value of $\chi_{xxxx}^{(3)}$ versus the concentration of the ZnTsPc-V-AQ solution measured at a pump intensity of $4.5 \times 10^6 \text{ W/cm}^2$ is shown in Fig. 4. From (1), we know that the linear dependence of the $\chi_{xxxx}^{(3)}$ on the concentration indicates that the pump pulse has

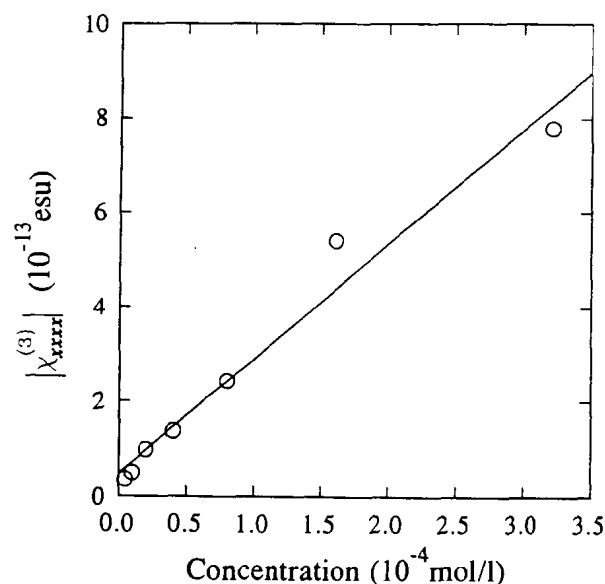


Fig. 4. Then value of $\chi_{xxxx}^{(3)}$ solution versus concentration measured at a pump intensity of $4.5 \times 10^6 \text{ W/cm}^2$. The solid line is a linear fit to the $\chi_{xxxx}^{(3)}$ data

Table 1. Molecular hyperpolarizability $\gamma_{ijk}(-\omega; \omega, \omega, -\omega)$ of ZnTsPc-V-AQ

$\langle \gamma_{xxxx}^g \rangle$	$\langle \gamma_{xxxx}^{CS} \rangle$	$\langle \gamma_{xyyx}^g \rangle$	$\langle \gamma_{xyyx}^{CS} \rangle$
$2.37 \times 10^{-31} \text{ esu}$	$2.46 \times 10^{-30} \text{ esu}$	$7.06 \times 10^{-32} \text{ esu}$	$7.02 \times 10^{-31} \text{ esu}$

saturated the population of the CS state. Therefore, the linear dependence shown in Fig. 4 means that the measurement was performed at a saturation pump intensity. Then a linear fit can yield the value of γ_{xxxx}^{CS} . The value of γ_{xyyx}^{CS} was also obtained in a similar way. Table 1 gives the molecular hyperpolarizabilities of the ground state and the CS state for parallel and perpendicular polarizations. Here we used the assumption $N_g = N_{CS} = N_0/2$ (N_0 is the total number density), which is valid at the saturation pump intensity because the lifetime [7] of the CS state of supra-molecules with porphyrin or phthalocyanine is usually much shorter than the laser pulse width of 8 ns. In addition, the ground-state hyperpolarizability, γ_{xxxx}^g , of ZnTsPc was determined to be $3.23 \times 10^{-31} \text{ esu}$. From Table 1, one can see that the CS-state hyperpolarizabilities of ZnTsPc-V-AQ were an order of magnitude larger than those of the ground state of ZnTsPc-V-AQ and the ground state of ZnTsPc.

3 Conclusion

We have observed that the molecular hyperpolarizability of a supra-molecule ZnTsPc-V-AQ was enhanced by ten times when the sample was optically pumped. By comparing the third-order NLO susceptibilities of assembled molecules with that of unassembled molecules, and measuring the ratio of the third-order NLO susceptibilities for parallel and perpendicular probe polarizations, we conclude that the enhancement of the third-order NLO susceptibility is due predominantly to population of the CS state with a large electronic molecular hyperpolarizability. It is verified that an excited state formed through charge transfer after optical excitation possesses a large molecular hyperpolarizability.

Acknowledgements. This research was supported by the National Natural Science Foundation of China.

References

1. D. Rogovin: Phys. Rev. Lett. **65**, 567 (1990)
2. Q.L. Zhou, J.R. Heflin, K.Y. Wong, O. Zamani-Khamiri, A.F. Garito: Phys. Rev. A **43**, 1673 (1991)
3. J.R. Heflin, D.C. Rodenberger, R.F. Shi, M. Wu, N.Q. Wang, Y.M. Cai, A.F. Garito: Phys. Rev. A **45**, R4233 (1992)
4. D.C. Rodenberger, J.R. Heflin, A.F. Garito: Nature **359**, 309 (1992)
5. N. Ooba, S. Tomwaru, T. Kurihara, T. Kaino, W. Yamada, M. Takagi, T. Yamamoto: Jpn. J. Appl. Phys. **34**, 3 139 Part 1(1995)
6. H.S. Nalwa, A. Kakuta, A. Mukoh: Chem. Phys. Lett. **203** 109 (1993)
7. F.J. Vergeldan, F.B.M. Koehorst, T.I. Schaafsma, J.-C. Lambry, J.-L. Martin, D.G. Johnson, M.R. Wasielewski: Chem. Phys. Lett. **182**, 107 (1991)
8. Y. Lin, K. Shigehara, M. Hra, A. Yamada: J. Am. Chem. Soc. **113**, 440 (1991)
9. I. Willner, J. Rosengaus, Y. Eichen: New J. Chem. **15**, 55 (1991)
10. D.J. McGraw, A.E. Siegman, G.M. Wallraff, R.D. Miller: Appl. Phys. Lett. **54**, 1713 (1989)
11. T.H. Tran-Thi, J.F. Lipskier, D. Houden, C. Penpin, E. Kenszei, J.P. Jay-Gerin: J. Chem. Soc. Faraday Trans **88**, 2129 (1992)

Photoinduced Intramolecular Electron Transfer in an Oblique Zinc Phthalocyanine - Viologen Linked System

Hong Jian TIAN, Qing Fu ZHOU, Hui Jun XU*

Institute of Photographic Chemistry, Academia Sinica, Beijing 100101

ABSTRACT: The spectroscopic properties and photoinduced electron transfer process have been studied in zinc phthalocyanine - viologen system with bisphenol A (ZnPcAV^{2+}). It was found that the excited singlet state of zinc phthalocyanine moiety is quenched and the fluorescence lifetime is reduced by the linked viologen. Nanosecond laser photolysis studies showed that intramolecular quenching of the excited triplet state of zinc phthalocyanine moiety by the attached viologen occurred giving reduced viologen radical ion ($\text{V}^{\cdot+}$) that survived over 50 μs .

The X-ray structure of the reaction center (RC) of photosynthetic bacterium in 1984¹ has initiated intense research in the design and syntheses of artificial synthetic models to mimic the primary photoinduced processes in the RC. Particularly interesting is the question related to the influence of mutual orientation of the chromophores on the photoinduced electron transfer and charge separation processes²⁻⁴. Recently, oblique bisporphyrins with 1,10-phenanthroline spacer group analogy with the mutual arrangements of various chromophores found in the RC have been synthesized to demonstrate the rapid photoinduced processes resemble the natural photosynthetic systems⁵. Previously, we synthesized a series of zinc phthalocyanine-viologen compounds covalently linked by a flexible alkoxy chain to study the effect of chain length on photoinduced electron transfer processes⁶. In this letter, we report the investigation of photoinduced intramolecular electron transfer process in an oblique zinc phthalocyanine-viologen system using bisphenol A as the spacer in attempting to understand the effect of mutual orientation of the donor-acceptor on the photoinduced process.

The structure of viologen-linked zinc phthalocyanine (ZnPcAV^{2+}) are shown in Fig.1. The synthesis of the compound will be reported elsewhere.

The absorption spectrum of ZnPcAV^{2+} and zinc phthalocyanine(ZnPcA) are similar. They showed very strong Q bands (681nm) with associated vibrational overtone(614nm) and strong B

bands(355nm). characteristic of the spectra of metal phthalocyanine. The parameters of electronic absorption spectra of the two compounds are given in Table 1. The results indicated the absence of any ground – state electronic interaction between the phthalocyanine moiety and the attached viologen.

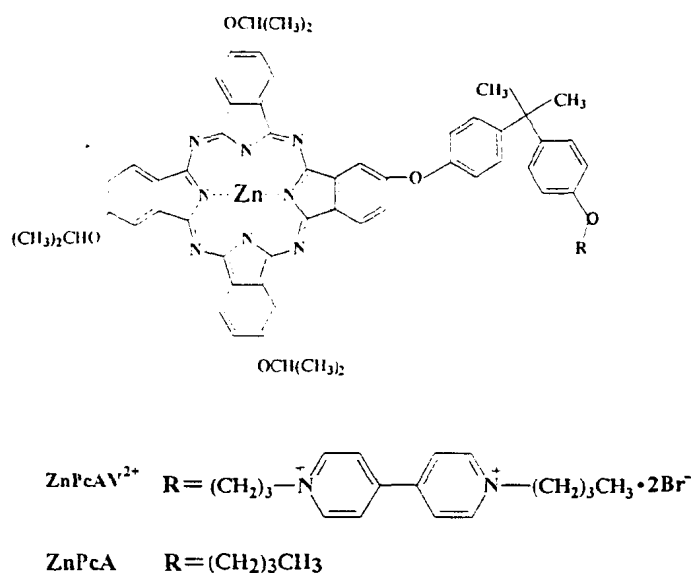


Figure 1. The structure of ZnPcAV²⁺ and ZnPcA

Table 1. Parameter of absorption of ZnPcAV²⁺ and ZnPcA in DMF

Compound	$\lambda_{\text{max}}/\text{nm} \text{ (log)}\epsilon$		
ZnPcAV ²⁺	681(5.27)	614(4.62)	355(4.96)
ZnPcA	681(5.30)	614(4.64)	355(4.97)

The fluorescence spectra of viologen-linked zinc phthalocyanine(ZnPcAV²⁺) and zinc phthalocyanine (ZnPcA) are shown in Fig.2. Although the shapes of the fluorescence spectra of these compound are almost the same, the fluorescence intensity of phthalocyanine are strongly affected by the viologen. In these experiments the concentration of the sample solution was adjusted in order to keep the absorbance at excited wavelength (605nm) constant for all sample solutions. The relative fluorescence intensity of ZnPcAV²⁺ is much lower compared with that of ZnPcA indicating that the photoexcited singlet state of phthalocyanine is quenched by the bonded viologen in ZnPcAV²⁺. It indicates that upon excitation the fluorescence of zinc phthalocyanine is appreciably quenched by the attached viologen. The total fluorescence quenching efficiency is estimated according to the following equation:

$$\Phi_q = (1 - \Phi_f/\Phi_f^0) \quad (1)$$

Here, Φ_f and Φ_f^0 are relative fluorescence quantum yields of ZnPc in ZnPcAV²⁺ and ZnPcA respectively.

The fluorescence lifetimes of ZnPc moiety in ZnPcAV²⁺ and ZnPcA are listed in Table 2. The lifetime of ZnPc in ZnPcAV²⁺ is shorter than that of ZnPc in ZnPcA. The fluorescence quenching efficiency can also be found from fluorescence life-time according to equation(2):

$$\Phi_D = (1 - \tau_f/\tau_f^0) \quad (2)$$

Here, τ and τ^0 is the fluorescence lifetimes of ZnPcAV²⁺ and ZnPcA respectively.

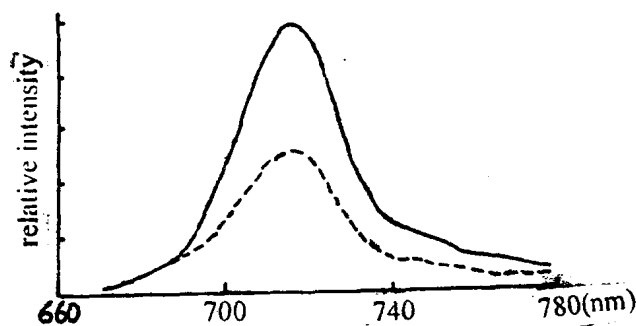


Fig.2 Fluorescence spectra of ZnPcAV²⁺ (—) and ZnPcA (- - -) in DMF (λ_{ex} =615nm)

Table 2. Photophysical properties of phthalocyanine linked viologen compound (ZnPcAV²⁺) and phthalocyanine (ZnPcA) in DMF solution

Compound	Φ_f	τ_f (ns)	Φ_q	Φ_D	$k_a (\times 10^7)$
ZnPcA	0.32	3.2			
ZnPcAV ²⁺	0.18	2.7	0.56	0.16	5.8

It is indicated that the fluorescence quenching efficiency from fluorescence quantum yield measurements are more than three-fold larger than those calculated from fluorescence life-time determinations. The observed difference in Q values is suggested to come from static quenching³. The quenching efficiency calculated from lifetime measurements is dynamic in nature responsible for electron transfer.

Intramolecular electron transfer rate constant(k_a) was calculated by the equation (3). The result is also included in Table 2.

$$k_a = 1/\tau - 1/\tau^0 \quad (3)$$

The transient absorption spectra of ZnPcAV²⁺ are shown in Figure 4. The broad transient absorption band in 440nm-600nm region is assigned to the excited triplet state of ZnPcA moiety. A

new absorption peak at 410nm which is observed in 5-20 μ s after excitation is attributed to the reduced viologen radical ($V^{\cdot+}$)⁷. The triplet state decayed and mostly disappeared in 20 μ s after laser excitation, however, the absorption due to $V^{\cdot+}$ still remained observable in 50 μ s after excitation.

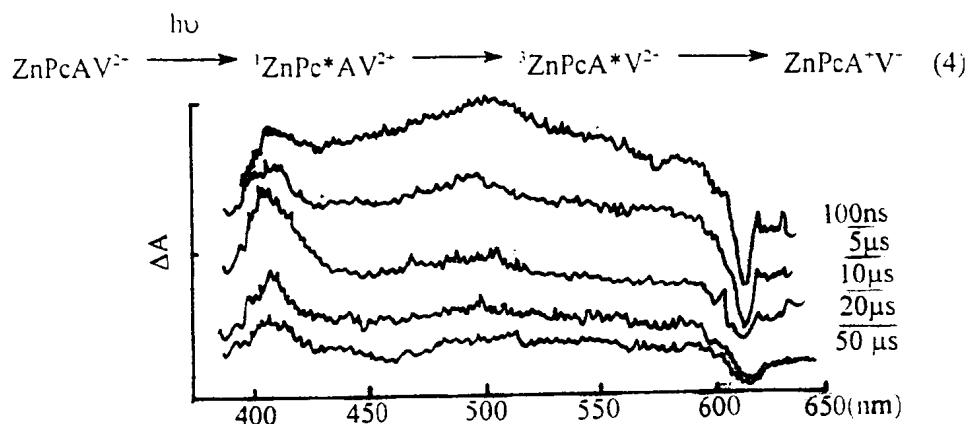


Fig.5 Transient absorption spectra observed on pulsed laser excitation of ZnPcAV^{2+} at 355nm in DMF

It is conceivable that there may be some extent of charge separation from an excited singlet state reaction, but our experimental limitation precluded its observation. It is noted that in this ZnPcAV^{2+} system the $V^{\cdot+}$ survived over 50 μ s duration which is shorter than that in the $\text{ZnPcC}_3\text{V}^{2+}$ system ($\sim 100\mu$ s)⁶. It is believed that the distance between the ZnPc moiety and V^{2+} linked to bisphenol A is very close to each other compared with that linked by a flexible alkoxy chain. A greater proximity between the two components involved in the electron transfer process in ZnPcAV^{2+} that enhances the reverse electron transfer and charge recombination.

Acknowledgment: This work is supported by the National Natural Science Foundation of China.

Reference:

1. J.Deisenhofer, H.Michel, *Angew. Chem., Int. Ed.Engl.* 1989,28,839.
2. A.Osuka, K.Maruyama, N.Mataga, T.Asahi, I.Yamuzaki, N.Tamai, *J.Am.Chem.Soc.*, 1990,112,4958.
3. A.Harriman, G.Porter, A.Wilowska, *J.Shem.Soc.,Faraday Trans. 2* 1984,80,191.
4. I.Okura, H.Hosono, *J.Phys.Chem.* 1993, 96,4466.
5. A.M.Burn, S.J.Atherton, A.Harriman, Veitz, J-P.Sauvage, *J.Am. Chem. Soc.*, 1992, 114,4632.
6. Y.Shen, J.X.Liu, Q.F.Zhou, H.J.Xu, *Chineses J.Chem.* 1995, 1, 33.
7. H.Ohtani, T.Kobayashi, T.Ohno, S.Kata, T.Tanno, A. Yamada, *J.Phy.Chem.*, 1984, 88, 4431.

(Received 22 April 1996)

新型卟啉-酞菁二元分子内光物理过程的研究*

李希友 田宏健 周庆复 许慧君

(中国科学院感光化学研究所, 北京 100101)

摘要 合成了以吡啶连接的含卟啉-酞菁的双发色团分子, 测定了它的吸收光谱, 荧光光谱和荧光寿命, 并计算了在不同溶剂中两发色团之间的能量传递效率 $\Phi_{\text{E} \rightarrow \text{T}}$ 和电子转移效率 Φ_{ET} . 结果表明: 在非极性溶剂苯中, 两发色团之间的光物理过程以激发态单线态能量传递为主 ($\Phi_{\text{E} \rightarrow \text{T}}$ 80%). 而在极性溶剂 DMF 中, 则以电子转移为主 (Φ_{ET} 69.8%). 该二元化合物在 DMF 中的电子转移效率明显高于我们以前合成的以氧或柔性链连接的二元化合物. 这可能是由于在 DMF 中, 吡啶以船式构象存在, 两个发色团呈较固定的, 相互平行的面对面构象. 从 CPK 分子模型可以算出卟啉环和酞菁环中心至中心的距离为 3.56 Å.

关键词: 吡啶, 二元化合物, 能量传递, 光诱导电子转移

人们为了模拟光合作用反应中心的原初过程, 设计合成了大量的含有多个发色团的模型化合物^[1], 研究此类化合物中各发色团间的激发态的能量传递和光诱导电子转移过程. Tran-Thi 等人^[2]和田宏健等人^[3]曾先后合成了以氧原子和以柔性链相连的卟啉-酞菁二元化合物并研究了连接链的性质, 链长和溶剂极性对上述光物理过程的影响. 为了研究二元化合物中两个发色团之间的相对取向对能量传递和电子转移的影响, 我们又设计合成了新的以吡啶相连的卟啉-酞菁二元化合物. 这种化合物的连接基 (spacer) 既有一定的刚性, 又能在一定的条件下实现几种稳定构象间的相互转化. 本文中我们分别用稳态荧光光谱和单光子计数技术研究了该化合物中卟啉、酞菁间的激发态能量传递和光诱导电子转移反应, 并讨论了环境条件和连接基构象变化对上述过程的影响.

1 实验部分

1.1 原料

四对甲基苯基卟啉 (TTP)、四异丙氧基酞菁 (H_2Pc) 及卟啉-酞菁 (Pr-Pc) 均为本室合成, 其合成方法将另文报导. 卟啉-酞菁 (Pr-Pc) 的结构式见下图. 二甲基甲酰胺 (DMF), 苯均为市售分析纯试剂. 经荧光检测无干扰荧光后使用.

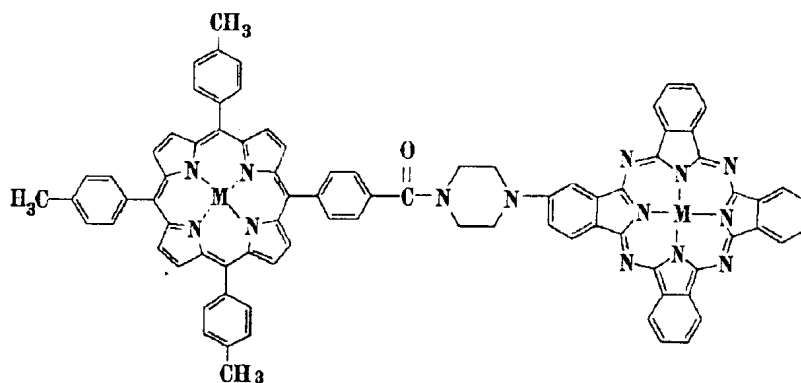
1.2 仪器及测试条件

吸收光谱: Hitachi 557 型紫外可见分光光度计

荧光光谱: Perkin-Elmer LS-5 荧光分光光度计, 配 3600 数据终端. 荧光寿命用 Horiba WAES-1100 单光子计数器.

1996-06-02 收到初稿, 1996-09-02 收到修改稿. 联系人: 许慧君. * 国家自然科学基金资助项目

测定光谱时样品浓度为: TTP $1 \times 10^{-5} \text{ mol} \cdot \text{L}^{-1}$; H_2Pc $2 \times 10^{-5} \text{ mol} \cdot \text{L}^{-1}$; Pr-Pc $1 \times 10^{-5} \text{ mol} \cdot \text{L}^{-1}$. 荧光寿命测定的样品需通氮气除氧 15 分钟后再用. 荧光量子产率以 TTP/苯 $\Phi=0.15^{[3a]}$, H_2Pc /苯 $\Phi=0.6^{[4]}$ 为标准, 全部实验在室温下进行.



式中: $M=2\text{H}$

Pr-Pc 的结构式

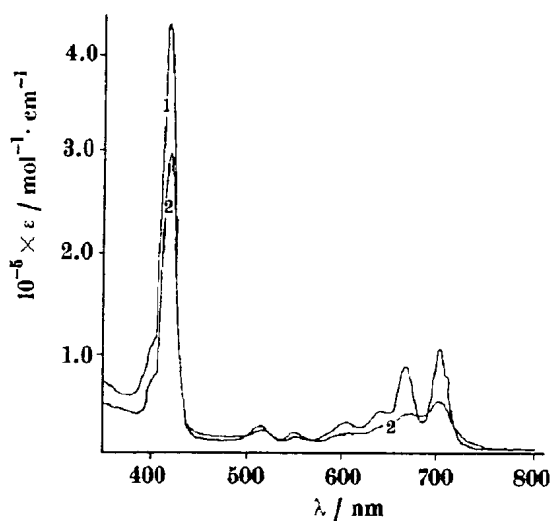


图 1 TTP, H_2Pc 等摩尔混合物及 Pr-Pc 在苯中的吸收光谱

Fig.1 Electronic absorption spectra of TTP, H_2Pc 1:1 mixture(1) and Pr-Pc(2) in benzene

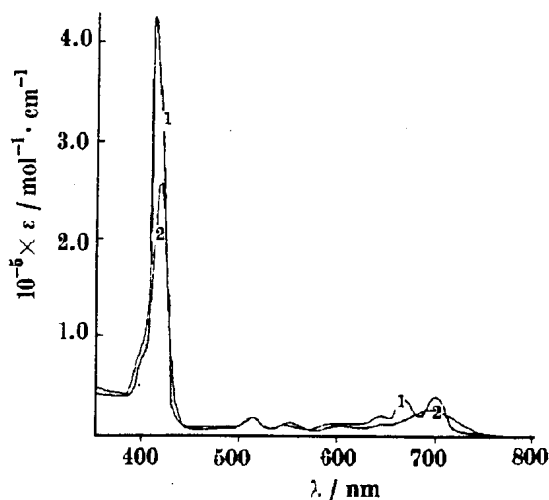


图 2 TTP, H_2Pc 等摩尔混合物及 Pr-Pc 在 DMF 中的吸收光谱

Fig.2 Electronic absorption spectra of TTP, H_2Pc 1:1 mixture(1) and Pr-Pc(2) in DMF

2 结果与讨论

2.1 稳态吸收光谱的研究

图 1,2 中所示为二元化合物和等摩尔 TTP、 H_2Pc 混合物的吸收光谱图, 由图中可以看出, 与等摩尔的 TTP、 H_2Pc 混合物相比, 二元化合物在苯中, 酞菁发色团的最大吸收波长稍向蓝移 3nm, 吸收强度也减小约 50%. 卟啉发色团的 B 带吸收强度比单分子的 B 带吸收下降了约 30%. 吸收谱的这些变化说明了二元化合物中, 两发色团之间在基态有弱的激子耦合作用. 在 DMF 中, 酞菁发色团的 660nm 处的吸收峰减小并变宽, 从而使得原来很明显的两个峰变为一个宽峰,

吸收强度也大幅度下降. 卟啉的 B 带吸收也下降约 30%. 吸收谱的这些变化较在苯中要大, 说明在 DMF 中, 两个基团间的作用比在苯中要大 (数据见表 1 所示).

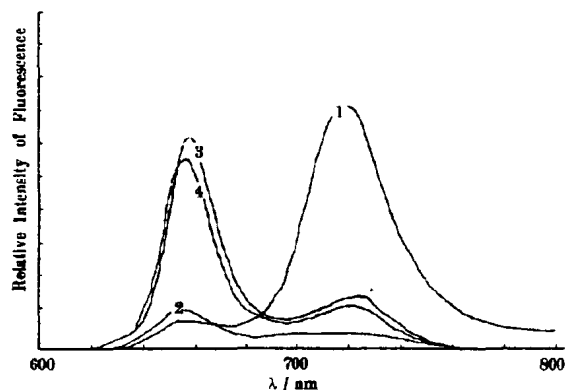


图 3 TTP 和 Pr-Pc 在苯中或 DMF 中的荧光光谱 ($\lambda_{EX}=515nm$)

Fig.3 The fluorescence spectra of TTP and Pr-Pc in benzene or DMF

1) Pr-Pc in benzene; 2) Pr-Pc in DMF; 3) TTP in benzene; 4) TTP in DMF

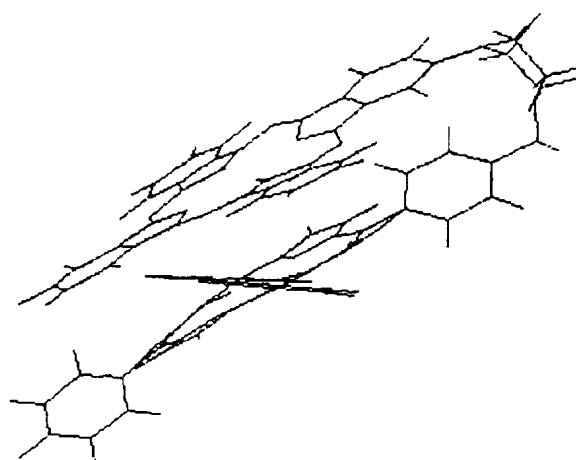


图 4 Pr-Pc 在 DMF 中的构象

Fig.4 The calculated conformation of Pr-Pc in DMF

2.2 能量传递的研究

能量传递效率取决于两个因素: 给体和受体的光谱交盖程度; 给体和受体在空间的相对位置 (距离和相对取向). 田宏健等人^[3a] 曾经计算了卟啉和酞菁的光谱的重叠积分和 Foster 能量传递临界距离 R_0 . 由这些数据可以看出, 卟啉和酞菁之间可以进行有效的能量传递. 我们分别在苯和 DMF 中, 选择性激发二元化合物中的卟啉 ($\lambda_{EX}=515nm$), 得到了它在 600–800nm 范围内的荧光光谱 (如图 3 所示). 由图中可以看出, 在苯中, 卟啉的荧光几乎全部被酞菁猝灭, 同时观察到酞菁在 710nm 处的强的荧光发射. 说明卟啉、酞菁之间发生了由卟啉到酞菁的单重态的分子内能量传递. 而在 DMF 中, 体系的荧光很弱, 说明体系中存在其它的光物理过程. 能量传递效率 Φ_{EnT} 可以通过如下公式 (1)^[5] 计算. 式中 F_D 和 F_A 分别是激发给体时二元分子的给体和受体的荧光光谱面积. Φ_D , Φ_A 分别是给体和受体的荧光量子产率, τ_D 是没有受体的给体的表现荧光寿命.

$$\Phi_{EnT} = \frac{\text{给体传递给受体的光子数}}{\text{给体吸收的光量子数}} = \frac{F_A / \Phi_A}{F_A / \Phi_A + F_D / \Phi_D} \quad (1)$$

根据式 (2)、(3) 可以计算卟啉荧光被酞菁猝灭的速率常数 k_q 和猝灭效率 Φ_q .

$$k_q = \tau_D^{-1} (\Phi_D / \Phi_{DA} - 1) \quad (2)$$

$$\Phi_q = \frac{k_q}{k_q + \tau_D^{-1}} \quad (3)$$

式中, Φ_{DA} 是二元分子中给体的荧光量子产率. 计算所得各值列于表 2 中. 由计算所得数据可以看出, 在苯中激发单重态能量传递效率 Φ_{EnT} 较荧光猝灭效率 Φ_q 小 10% 左右, 说明苯中单重态的能量传递过程是主要的光物理过程, 但仍有少量其它光物理过程存在. 从表 2 中的数据还可以看出, 溶剂的极性对能量传递的效率有很大的影响. 在 DMF 中, 激发单重态的能量传递不再是主要过程, Φ_{EnT} 仅为 6%, 而 Φ_q 为 70.5%, 这表明在分子内其它的光物理过程占主导地位. 我们认为可能是卟啉和酞菁之间发生了电子转移反应.

表 1 有关化合物的光物理常数

Table 1 The photophysical constants of related compounds					
compounds	solvent	fluorescence spectra		absorption spectra	
		$\Phi_f(\%)$	τ_f/ns	$\lambda/\text{nm}(\epsilon L/\text{mol}\cdot\text{cm}^{-1})$	
TTP	benzene	0.15	11.7 ^a	420(4.4×10^5);	516(3.4×10^4)
	DMF	0.14	11.7 ^a	420(4.2×10^5);	516(2.2×10^4)
H ₂ Pc	benzene	0.6	6.8 ^b	706(9.7×10^4);	670(8.1×10^4)
	DMF	0.55	6.0 ^b	641(3.06×10^4);	607(1.99×10^4)
Pr-Pc	benzene	0.41(0.022 ^d)	6.0 ^c	706(6.2×10^4);	673(5.8×10^4)
				644(2.2×10^4);	612(1.5×10^4)
	DMF	0.064(0.032 ^d)	2.2 ^c	702(6.0×10^4);	669(4.5×10^4)
				515(3.22×10^4);	420(3.0×10^5)
				703(4.48×10^4);	515(2.02×10^4)
				420(2.5×10^5)	

a) Excited wavelength (λ_{EX})515nm; Emission wavelength(λ_{EM}) 660nmb) Excited wavelength (λ_{EX})615nm; Emission wavelength(λ_{EM}) 710nmc) Excited wavelength (λ_{EX})515nm; Emission wavelength (λ_{EM}) 710nm

d) The quantum yield of porphyrin of the heterodimer

2.3 光诱导电子转移反应的研究

根据卟啉和酞菁的氧化还原电位可以计算它们之间的电子转移反应的自由能变化 ΔG^0 [3a]。根据计算, 卟啉作为电子给体, 酞菁作为电子受体时 $\Delta G^0 = -0.12\text{eV}$ [3a], 是热力学允许的反应。我们以 615nm 的光激发二元化合物, 测得它在苯和 DMF 中的酞菁的表现荧光寿命, 然后根据公式 (4) 和 (5) 可以计算得到酞菁和卟啉之间的电子转移速率常数 k_{ET} 和电子转移效率 Φ_{ET} 。式中 τ_f 为二元化合物中受体的表现荧光寿命, τ_f^0 为受体模型化合物的表现荧光寿命。结果列于表 3 中

表 2 二元化合物中的能量传递物理常数

Table 2 The energy transfer constants of the heterodimer					
solvent	$J^a/\text{mol}^{-1}\cdot\text{cm}^{-1}$	$R_0^a/\text{\AA}$	$\Phi_{\text{ET}}(\%)$	$\Phi_q(\%)$	$k_q(\times 10^8)$
benzene	1.6×10^{-12}	58.2	75	80.9	4.97
DMF	1.13×10^{-12}	52.3	6	70.5	2.8

a. Data from reference [3a]

$$k_{\text{ET}} = 1/\tau_f - 1/\tau_f^0 \quad (4)$$

$$\Phi_{\text{ET}} = k_{\text{ET}}/(k_{\text{ET}} + 1/\tau_f^0) \quad (5)$$

表 3 二元化合物的电子转移物理常数

Table 3 The photoinduced electron transfer constants of the heterodimer				
compound	solvent	τ_f^a/ns	$\Phi_{\text{ET}}(\%)$	$k_{\text{ET}}/\text{s}^{-1}$
H ₂ Pc	benzene	6.8	—	—
	DMF	6.0	—	—
Pr-Pc	benzene	6.0	11	1.9×10^7
	DMF	2.1	69.8	3.3×10^8

a) Excited wavelength (λ_{EX}) 615nm, Emission wavelength (λ_{EM}) 710nm

由表中数据可以看出, 在 DMF 中光诱导电子转移效率高达 69.8%, 说明在 DMF 中电子转移是主要的光物理过程, 其它过程无法与它竞争。用此数值和我们以前合成的以氧 [3a] 和柔性链 [3b] 连接的二元化合物的电子转移效率相比, 它也要高出许多。我们认为这是哌嗪的特殊构象造成的

吡啶在 DMF 中受光激发时可能主要以船式构象存在, 我们用 CPK 分子模型对其结构进行了模拟, 结果发现吡啶和酞菁呈相互平行的面对面的构象(图 4 所示), 两环中心至中心的距离为 3.56Å. 这种构象中, 吡啶和酞菁之间的电子云有很大的交盖, 因此能够进行很快的电子转移反应, 这也可以解释它的吸收光谱的变化较大和体系的荧光很弱等现象. 比较表 2 和表 3 中的 Φ_{EnT} , Φ_{ET} 和 Φ_{Q} 三个数据还可以看出, Φ_{EnT} 和 Φ_{ET} 相加接近于 Φ_{Q} , 这再一次说明该二元化合物中, 吡啶的荧光的猝灭主要是由光诱导电子转移和激发态的能量传递造成的.

参 考 文 献

- 1 (a) Boxer S G, Closs G L. *J. Am. Chem. Soc.*, **1976**, **98**:5406
 (b) Bucks R R, Boxer S G. *J. Am. Chem. Soc.*, **1982**, **104**:340
 (c) Tsuyoshi Asahi. *J. Am. Chem. Soc.*, **1993**, **115**: 5665
 (d) Collman J P. *J. Org. Chem.*, **1995**, **60**:1926
 (e) Johnson D G. *J. Am. Chem. Soc.*, **1993**, **115**:5692
 (f) Brookfield R L. *J. Chem. Soc., Faraday Trans.* **1985**, **2**, **81**:1837
- 2 Tran-Thi T H. *J. Phys. Chem.*, **1989**, **93**:1226
- 3 (a) Tian H J, Zhou Q F, Shen S Y, Xu H J. *J. Photochem. Photobiol. A: Chem.*, **1993**, **720**:163
 (b) 周庆复, 田宏健, 沈淑引, 许慧君. *感光科学与光化学*, **1992**, **10**:144
 (c) Tian H J, Zhou Q F, Shen S Y, Xu H J. *Chin. Chem. Lett.*, **1992** **3**(11): 873
- 4 Xu H J, Xiong G X. *J. Photochem. Photobiol. A: Chem.*, **1995**, **92**:35
- 5 田宏健. 中国科学院感光化学研究所博士论文, 1994,7

The Photophysical Process of A New Kind of Porphyrin-Phthalocyanine Heterodimer

Li Xiyou Tian Hongjian Zhou Qingfu Xu Huijun

(Institute of Potographic Chemistry, Academia Sinica, Beijing 100101)

Abstract Intramolecular energy-transfer and electron-transfer of porphyrin-phthalocyanine heterodimer, linked by piperazine, were investigated by absorption and fluorescence spectroscopy. The efficiency of energy transfer(Φ_{EnT}) and electron transfer (Φ_{ET}) were calculated. The results indicate that: In benzene, the main photophysical process is excited singlet-singlet energy transfer, while in DMF photoinduced electron transfer predominant. The Φ_{ET} of this heterodimer in DMF is bigger than that of porphyrin-phthalocyanine heterodimers linked by oxygen or flexible chains. This may be ascribed to the "boat-form" conformation of piperazine, According to the CPK molecular model, porphyrin and phthalocyanine are held together in a face to face way, and the center to center distance between two macrorings is about 3.56Å. It is suggested that conformational changes from "chair form" to "boat form" occurred subsequent to optical excitation in DMF.

Keywords: Piperazine, Heterodimer, Intramolecular energy transfer, Photoinduced electron transfer

共吸附对卟啉、酞菁/二氧化钛复合电极光电特性的影响*

毛海舫 田宏健 周庆复 许慧君

(中国科学院感光化学研究所, 北京, 100101)

沈耀春 陆祖宏

(东南大学分子与生物分子电子学国家实验室, 南京, 210018)

摘要 制备了ZnTSP/TiO₂、GaTSPc/TiO₂和共吸附ZnTSP、GaTSPc/TiO₂电极,并研究了它们的光电特性。结果表明,共吸附的ZnTSP、GaTSPc/TiO₂电极不仅拓宽了光电响应范围,而且提高了光电转换效率,特别是提高了GaTSPc的光电转换效率。其原因可能是GaTSPc的聚集体没有敏化作用,而卟啉和酞菁分子与TiO₂共吸附可以减少GaTSPc的聚集,有效地增强了GaTSPc的敏化能力。

关键词 卟啉,酞菁,二氧化钛,超微粒,光电流

用有机染料敏化带隙较宽的半导体研制的有机光化学电池^[1],其转换效率不够理想。Gratzel等^[2]用二氧化钛超微粒制备的多孔电极,由于其比表面积大,电极表面能吸附较多的染料分子,因而光电转换效率大大提高。卟啉、酞菁化合物在可见光范围内有强吸收,两者吸收光谱叠加基本覆盖了可见光的所有波长范围,而且卟啉、酞菁化合物有良好的光、热稳定性,是较好的光敏染料。因此,研究由卟啉、酞菁和二氧化钛组成的有机-无机复合电极十分有意义。

本文着重研究了共吸附对卟啉、酞菁/二氧化钛共吸附电极光电响应特性的影响。结果表明,与卟啉/二氧化钛、酞菁/二氧化钛单一染料敏化的电极相比,共吸附不仅能拓宽光电响应范围,而且能提高光电转换效率。

1 实 验

1.1 原 料

自制中位-四-(对磺酸基-苯基)锌卟啉(ZnTSP),2,9,16,23-四磺化镓酞菁(GaTSPc)由扬州师范大学提供,均纯化后经元素分析鉴定合格。

TiO₂超微粒通过水解钛酸异丙酯制得^[3]。使用前渗析除去异丙醇,调pH值为2.5。使用时胶体浓度为0.1 mol/L,透射电镜测得其粒径为5 nm左右。

磺化酞菁/TiO₂的电极根据文献^[4]方法制备,在按不同比例混合的ZnTSP、GaTSPc的混合溶液中吸附24 h,则得到ZnTSP、GaTSPc共吸附的复合电极。

1.2 仪 器

UV-Vis 2201 紫外可见光谱仪(日本岛津);原子力显微镜(DI公司的Nanoscope III 仪器);CBMP-1 型双恒电位仪;光源为高压氙灯;WPG3D 光栅单色仪;FP-3 型光密度计;电

收稿日期:1996-02-10。联系人及第一作者:毛海舫,男,35岁,博士,助理研究员,现在中国科学院感光化学研究所工作。

* 国家自然科学基金资助项目。